# Inverse Dynamics Control of Bimanual Object Manipulation Using Orthogonal Decomposition: An Analytic Approach

Mohammad Shahbazi, Jinoh Lee, Darwin Caldwell, and Nikolaos Tsagarakis

***Abstract*— In this paper, the well-known problem of codependence between inverse dynamics torque and contact force in bimanual object manipulation is addressed. The common contact constraint, namely rigid grasping, is exploited to decompose the set of dynamics equations into two orthogonally decoupled sets. Subsequently, the inverse dynamics control is formulated in a sub-manifold that is independent of the contact force, leading to analytically correct solutions that do not need to resort to common approximations for the aforementioned codependence problem. The contact force is also analytically computed and, therefore, can be optimally distributed using the torque redundancy. Relying on this prediction is most significant in situations where a force sensor at the end-effector is not present or is faulty. Even in the availability of sensory data, the predicted force may be used to correct typically noisy or delayed when filtered measurements, resulting in improved robustness. Simulation experiments on a planar bimanual manipulation model are presented.**

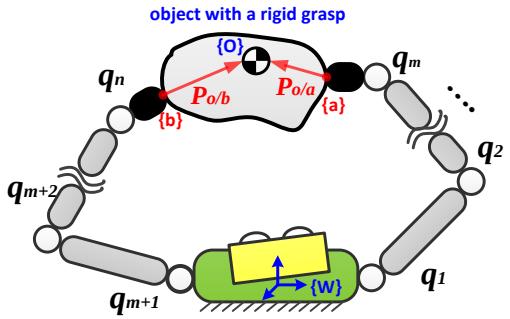


Fig. 1. A schematic diagram of the bimanual manipulation of a common object, where the detailed symbol representations are indicated in Section II.

## I. Introduction

In the past three decades, there has been much research in the control of bimanual robotic systems, because two arms performing a task together in a coordinated manner have a significant advantage over a single robot just as a human being using two arms has an advantage over on using one arm [1]–[4]. Recently, there has been a remarkable advent of many anthropomorphic robots with two arms in both service robots including humanoids as well as industrial robots such as Yumi (ABB), Nextage (Kawada), SDA-series (Motoman) and Baxter (Rethink). This promotes the researchers redraw attention on the bimanual control problem to develop more practical methods applicable even outside of a laboratory environment.

Of a large number of robotic tasks which the dual arm robot can perform, manipulating a common object is considered as an important application, since it includes a transportation of a heavy, large, and irregular-shaped object [5]. In this case, it is assumed that two arms rigidly hold the object; thus, the kinematic interrelation between two arms is not changed and they form a closed kinematic chain as shown in Fig. 1. Particularly, the kinematic constraints in this bimanual manipulation setup introduce actuation redundancy, since the number of the actuator can be more than the number of the independent task variables [6]. This redundancy is beneficial to improve dexterity of the system [7], so that internal (or squeeze) forces and dynamic load distribution [8] have been exploited with hybrid force/position [9] and impedance control [10] incorporating to advanced control methods such as sliding mode, robust adaptive law, and neural-network [4].

However, despite aforementioned successful studies so far, it is well-known that the codependency of constraint forces and control commands and the additional object dynamics and kinematic constraints in bimanual system induce considerable complexity in control. Moreover, the force control is imperative in dynamic coordinative manipulation, because the object is manipulated by the work done by interaction forces between the end-effectors. Force control should be done along the direction in which the end-effector moves. Therefore, the bimanual robot needs force-torque sensors or any dynamic observers to approximate the interaction forces which is often imprecise.

To alleviate the aforementioned limitations, this paper proposes a novel bimanual control framework for an object manipulation. First, a compact representation of bimanual robot and object dynamics is derived in the same form as that of conventional manipulators, where the kinematic constraint of the contact under the rigid grasping condition is exploited to decompose the set of dynamics equations into two orthogonally decoupled sets [11]. The orthogonal decomposition method has been introduced in legged locomotion [12], yet it is not straightforward to implement into the bimanual system. In this paper, we further extend the method to be applicable to the bimanual object manipulation task.

Second, having determined the inverse dynamics torque in the constraint compatible sub-manifold, the constraint force is analytically calculated and, therefore, can be optimally distributed without force sensors or common approximations

The research leading to these results has received funding from the European Union's Horizon 2020 research and innovation programme under the grant agreement No 644839 (CENTAURO). The authors are with Department of Advanced Robotics, Istituto Italiano di Tecnologia (IIT), Via Morego 30, 16163, Genova, Italy. {mohammad.shahbazi, jinoh.lee, darwin.caldwell, nikos.tsagarakis}@iit.it

methods. This is not trivial because the analytic solution of the interaction forces is valid in situations where a force sensor at the end-effector is not present or is faulty. Even in the availability of sensory data, the calculated force can be used to correct typically noisy or delayed when filtered measurements, which improves robustness of the closed loop system against uncertainties.

The rest of the paper proceeds as follows. Section II presents the compact dynamic equations formulated to establish the control scenario of bimanual manipulation of an object. Section III proposes inverse dynamic control with analytic solutions for both control commands and constraint forces via orthogonal decomposition. To improve control robustness against a use of object dynamics information, a practical online dynamics compensation method is also introduced. Performance of the developed controllers is illustrated on a simulated planar dual arm setup in Section IV, and numerical evaluation results are presented. And lastly, Section V presents the conclusion of this work.

## II. Bimanual Manipulation Dynamics

Consider a system of two arms affixed to ground as illustrated in Fig. 1. The arms *rigidly* grasp an undeformable object. The equations of motion for the dual arm robot can be written in the following compact form:

$$M(q)\ddot{q} + h(q,\dot{q}) = S^{\mathrm{T}}\tau + J^{\mathrm{T}}(q)\lambda, \tag{1}$$

where $q \in \mathbb{R}^n$ is the vector of generalized coordinates for $n$ joints, $M(q) \in \mathbb{R}^{n\times n}$ is the inertial matrix, $h(q,\dot{q}) \in \mathbb{R}^n$ is the vector of generalized centripetal, Coriolis, and gravity forces, $S \in \mathbb{R}^{n\times n}$ is the actuated joint selection matrix, and $\tau \in \mathbb{R}^n$ is the vector of torques (or control commands). Let $J_i(q) \in \mathbb{R}^{k\times n}$, $i \in \{\mathrm{a},\mathrm{b}\}$, with $k$ linearly independent contact constraints, be the Jacobian mapping the generalized velocities onto the vector of linear and angular velocities of the end-effectors, and $\lambda_i \in \mathbb{R}^k$ be the vector of forces and torques applied by the object on the corresponding end-effector. Accordingly, $J(q) = \begin{bmatrix} J_{\mathrm{a}}^{\mathrm{T}}(q) & J_{\mathrm{b}}^{\mathrm{T}}(q) \end{bmatrix}^{\mathrm{T}}$ and $\lambda = \begin{bmatrix} \lambda_{\mathrm{a}}^{\mathrm{T}} & \lambda_{\mathrm{b}}^{\mathrm{T}} \end{bmatrix}^{\mathrm{T}}$.

The equation of motion for the object is then given as

$$M_{\mathrm{o}}\dot{v}_{\mathrm{o}} + h_{\mathrm{o}}(z_{\mathrm{o}}, v_{\mathrm{o}}) = -G_{\mathrm{o}}^{\mathrm{T}}(z_{\mathrm{o}})\lambda, \tag{2}$$

in which $z_{\mathrm{o}} = \begin{bmatrix} p_{\mathrm{o}}^{\mathrm{T}} & \phi_{\mathrm{o}}^{\mathrm{T}} \end{bmatrix}^{\mathrm{T}} \in \mathbb{R}^k$ is the vector of position and minimal representation of the orientation of the object's center of mass (CoM), $v_{\mathrm{o}} = \begin{bmatrix} \dot{p}_{\mathrm{o}}^{\mathrm{T}} & \omega_{\mathrm{o}}^{\mathrm{T}} \end{bmatrix}^{\mathrm{T}}$ is the corresponding velocity vector ($v_{\mathrm{o}} = T(z_{\mathrm{o}})\dot{z}_{\mathrm{o}}$, with $T(z_{\mathrm{o}})$ being a transformation matrix, e.g., $T(z_{\mathrm{o}}) = I_k$ for the planar case; please refer to [13] for the definition.), $M_{\mathrm{o}} \in \mathbb{R}^{k\times k}$ is the object inertial matrix, $h_{\mathrm{o}}(z_{\mathrm{o}}, v_{\mathrm{o}}) \in \mathbb{R}^k$ is the vector of generalized centripetal, Coriolis, and gravity forces, $G_{\mathrm{o}}(z_{\mathrm{o}}) = \begin{bmatrix} G_{\mathrm{oa}}^{\mathrm{T}}(z_{\mathrm{o}}) & G_{\mathrm{ob}}^{\mathrm{T}}(z_{\mathrm{o}}) \end{bmatrix}^{\mathrm{T}}$ is the grasp matrix, and $G_{oi}(z_{\mathrm{o}}) \in \mathbb{R}^{k\times k}$, $i \in \{\mathrm{a},\mathrm{b}\}$, is a transformation matrix which maps the velocities of the object onto the velocities of the corresponding end-effector given as

$$G_{oi}(z_{\mathrm{o}}) = \begin{bmatrix} I & p_{o/i}\times \\ 0 & I \end{bmatrix}. \tag{3}$$

$p_{o/i}$ is the position vector of the object relative to the end-effector $i$, and $\times$ denotes the cross product in a coordinate representation. Finally, the rigid grasping constraints at the position and velocity levels can be represented by

$$z_{\mathrm{o}} = \mathrm{fk}_{\mathrm{a}}(q) = \mathrm{fk}_{\mathrm{b}}(q), \tag{4}$$

$$v_{\mathrm{o}} = G_{\mathrm{oa}}^{-1}J_{\mathrm{a}}\dot{q} = G_{\mathrm{ob}}^{-1}J_{\mathrm{b}}\dot{q}, \tag{5}$$

where $\mathrm{fk}_i(q)$ is the forward kinematics of the end-effector $i$. Hereinafter, the function arguments are suppressed for convenience unless necessary.

We now reformulate the above derivations such that they can be later exploited for the purpose of control. Starting from (5), it is straightforward to show that

$$J_{\mathrm{g}}\dot{q} = 0, \tag{6}$$

with

$$J_{\mathrm{g}} = J_{\mathrm{a}} - G_{\mathrm{oa}}G_{\mathrm{ob}}^{-1}J_{\mathrm{b}}. \tag{7}$$

We refer to $J_{\mathrm{g}}$ as the *grasp* Jacobian. Notice the difference between the grasp matrix $G_{\mathrm{o}}$, as constructed using (3) for the grasp points, and the proposed grasp Jacobian $J_{\mathrm{g}}$, as defined in (7). One can see that the property (6) holds if the grasp condition is rigid,

Next, by substituting for $\lambda_{\mathrm{b}}$ in (1) its corresponding expression from (2), i.e., $\lambda_{\mathrm{b}} = -G_{\mathrm{ob}}^{-\mathrm{T}}\left(G_{\mathrm{oa}}^{\mathrm{T}}\lambda_{\mathrm{a}} + M_{\mathrm{o}}\dot{v}_{\mathrm{o}} + h_{\mathrm{o}}\right)$, and observing that from (5) we have $\dot{v}_{\mathrm{o}} = G_{\mathrm{ob}}^{-1}J_{\mathrm{b}}\ddot{q} + G_{\mathrm{ob}}^{-1}\left(\dot{J}_{\mathrm{b}} - \dot{G}_{\mathrm{ob}}G_{\mathrm{ob}}^{-1}J_{\mathrm{b}}\right)\dot{q}$, the combined equations of motion are obtained as

$$\hat{M}\ddot{q} + \hat{h} = S^{\mathrm{T}}\tau + J_{\mathrm{g}}^{\mathrm{T}}\lambda_{\mathrm{a}}, \tag{8}$$

in which

$$\hat{M} = M + J_{\mathrm{b}}^{\mathrm{T}}G_{\mathrm{ob}}^{-\mathrm{T}}M_{\mathrm{o}}G_{\mathrm{ob}}^{-1}J_{\mathrm{b}},$$

$$\hat{h} = h + J_{\mathrm{b}}^{\mathrm{T}}G_{\mathrm{ob}}^{-\mathrm{T}}\left(h_{\mathrm{o}} + M_{\mathrm{o}}G_{\mathrm{ob}}^{-1}\left(\dot{J}_{\mathrm{b}} - \dot{G}_{\mathrm{ob}}G_{\mathrm{ob}}^{-1}J_{\mathrm{b}}\right)\dot{q}\right),$$

and $\bullet^{-\mathrm{T}}$ denotes an inverse transpose of $\bullet$. The dynamics representation (8) together with the grasp constraint (6) offers a compact form for the bimanual manipulation dynamics that resembles the classical constrained dynamics formulations. In the classical form, the geometric Jacobian of the contact points is used in the form of (6) to describe the constraint types in which no motion is observed in the constrained dimensions with respect to the inertial frame. Here we have obtained a similar form, but based on the grasp Jacobian $J_{\mathrm{g}}$, to represent the rigid grasping, i.e., when no relative motion is observed between two arms at the grasp points.

This result sets a new stage for the development of control strategies for bimanual manipulation by leveraging on the state-of-the-art methods originally proposed for other robotic applications with similar constrained dynamics representations, e.g., legged locomotion. In the following section, we extend one of those methods to develop analytically correct and efficient inverse dynamics solutions for the bimanual object manipulation that can minimize any combination of quadratic and linear costs in control command and constraint force.

## III. Bimanual Manipulation Control

We start by observing that there is a codependence between the control command $\tau$ and the constraint force $\lambda_{\mathrm{a}}$ in (8), which prevents a direct calculation of the inverse dynamics torque, if force sensors in all constraint dimensions do not exist. Even by assuming the presence of sufficiently accurate and smooth sensory data, the torque redundancy can no longer be used to shape the constraint forces, because they are approximated by the measured forces.

### A. Inverse dynamics via orthogonal decomposition

To resolve the aforementioned issue, the constrained dynamics can be projected onto a sub-manifold that is constraint consistent [11], [12], [14], and therefore independent of the constraint forces, as long as the rigid grasping condition is met, i.e., $J_{\mathrm{g}}\dot{q} = 0$. In general, the reduced number of equations can be written as

$$P\left(\hat{M}\ddot{q} + \hat{h}\right) = PS^{\mathrm{T}}\tau, \tag{9}$$

in which $P$ is a linear projector of rank $n-k$. Subsequently, the inverse dynamics torque can be calculated as follows [15]:

$$\begin{aligned}\tau(W,\tau_0) = &\left(PS^{\mathrm{T}}\right)^{\#} P\left(\hat{M}\ddot{q}_{\mathrm{des}} + \hat{h}\right)\\ &+ \left(I - (PS^{\mathrm{T}})^{\#}PS^{\mathrm{T}}\right)W^{-1}\tau_0,\end{aligned} \tag{10}$$

where $W$ is a symmetric positive definite matrix, $\tau_0$ is an arbitrary torque vector, $\bullet^{\#}$ denotes a $W$-weighted generalized inverse of $\bullet$, such that

$$(PS^{\mathrm{T}})^{\#} \triangleq W^{-\frac{1}{2}}\left(PS^{\mathrm{T}}W^{-\frac{1}{2}}\right)^{+},$$

and $\ddot{q}_{\mathrm{des}}$ is a desired constraint consistent joint acceleration vector.

As shown in [15], the choice of $P$ does not affect the calculated control signals, and is only important with respect to computational issues[1]. An effective way of constructing such operator is to use orthogonal decomposition technique as in [12], [16]. Following the method developed in [12], the projector can be constructed as

$$P_{\mathrm{QR}} = \hat{S}_{\mathrm{u}}\hat{Q}^{\mathrm{T}}, \tag{11}$$

where $\hat{Q}$ is determined from the QR decomposition of the transposed grasp Jacobian, i.e., $J_{\mathrm{g}}^{\mathrm{T}} = \hat{Q}\begin{bmatrix}\hat{R}^{\mathrm{T}} & 0\end{bmatrix}^{\mathrm{T}}$, and $\hat{S}_{\mathrm{u}} = \begin{bmatrix}0_{(n-k)\times k} & I_{(n-k)}\end{bmatrix}$ is a selection matrix. Notice that $P_{\mathrm{QR}}$ is a purely kinematic operator.

Having determined the inverse dynamics torque $\tau$, the contact force exerted by the manipulated object on the end-effector 'a' can be computed by

$$\lambda_{\mathrm{a}} = \hat{R}^{-1}\hat{S}_{\mathrm{c}}\hat{Q}^{\mathrm{T}}\left(\hat{M}\ddot{q}_{\mathrm{des}} + \hat{h} - S^{\mathrm{T}}\tau\right), \tag{12}$$

with $\hat{S}_{\mathrm{c}} = \begin{bmatrix}I_k & 0_{k\times(n-k)}\end{bmatrix}$. Finally, one can solve (2) for $\lambda_{\mathrm{b}}$ with the derived value for $\lambda_{\mathrm{a}}$.

[1]Examples of $P$ include [11] $P_{\mathrm{J}} = I - J_{\mathrm{g}}^{+}J_{\mathrm{g}}$, and $P_{\mathrm{M}} = I - J_{\mathrm{g}}^{\mathrm{T}}(J_{\mathrm{g}}\hat{M}^{-1}J_{\mathrm{g}}^{\mathrm{T}})^{-1}J_{\mathrm{g}}\hat{M}^{-1}$.

### B. Minimizing costs in control command and contact force

The inverse dynamics torque (10) is parameterized by $W$ and $\tau_0$. It is indeed the adjustment of these parameters that resolves the torque redundancy. In the following, we show how they can be used to minimize quadratic and linear costs in control command and constraint force.

*1) Minimizing control torque command:*

*Theorem 1 ( [15, Th 3.1]):* Given a symmetric positive definite matrix $W_\tau$ and an arbitrary vector $b_\tau$, the controller that minimizes the cost

$$\frac{1}{2}\tau^{\mathrm{T}}W_\tau\tau + b_\tau^{\mathrm{T}}\tau \tag{13}$$

at each instant of time and achieves the desired constraint compatible accelerations is selected by choosing

$$\begin{aligned}W &= W_\tau\\ \tau_0 &= -b_\tau.\end{aligned}$$

Therefore, one can observe that the inverse dynamics torque (10) without the null-space term, i.e., $\tau(W) = \left(PS^{\mathrm{T}}\right)^{\#}P\left(\hat{M}\ddot{q}_{\mathrm{des}} + \hat{h}\right)$, minimizes the quadratic cost $\frac{1}{2}\tau^{\mathrm{T}}W\tau$ in the control command.

*2) Minimizing constraint force:* Given the control command $\tau$, in order to minimize the constraint force $\lambda$ it is convenient to first solve (1) for $\lambda$. Depending on the number of joints and constraints, the resulting linear system can be either determined or overdetermined. In the latter case, one can use the QR decomposition of the end-effector geometric Jacobian, $J^{\mathrm{T}} = Q\begin{bmatrix}R^{\mathrm{T}} & 0\end{bmatrix}^{\mathrm{T}}$, to extract the $2k$ linearly independent equations that provide the unique solution of $\lambda$ given as

$$\lambda = R^{-1}S_{\mathrm{c}}Q^{\mathrm{T}}\left(M\ddot{q}_{\mathrm{des}} + h - S^{\mathrm{T}}\tau\right). \tag{14}$$

Using (14), it is straightforward to show that minimizing the cost $\frac{1}{2}\lambda^{\mathrm{T}}W_\lambda\lambda$ in the constraint force is equivalent to minimizing (13) with the following parameters:

$$W_\tau = SW_{\mathrm{c}}S^{\mathrm{T}}, \quad b_\tau = -SW_{\mathrm{c}}(M\ddot{q}_{\mathrm{des}} + h), \tag{15}$$

in which

$$W_{\mathrm{c}} = QS_{\mathrm{c}}^{\mathrm{T}}R^{-\mathrm{T}}W_\lambda R^{-1}S_{\mathrm{c}}Q^{\mathrm{T}},$$

and, therefore, the result of Theorem 1 is applicable.

As common in the cooperative manipulation literature, it may be useful to decompose the constraint force into motion-inducing $\lambda_{\mathrm{m}}$ and internal (or squeeze) $\lambda_{\mathrm{s}}$ force [10], which can be obtained by the following decomposition:

$$\lambda_{\mathrm{m}} = G_{\mathrm{o}}^{\mathrm{T}\#}G_{\mathrm{o}}^{\mathrm{T}}\lambda, \quad \lambda_{\mathrm{s}} = \left(I - G_{\mathrm{o}}^{\mathrm{T}\#}G_{\mathrm{o}}^{\mathrm{T}}\right)\lambda. \tag{16}$$

Since the squeeze force $\lambda_{\mathrm{s}}$ lies in the null-space of $G_{\mathrm{o}}^{\mathrm{T}}$, it produces no net force on the object; however, it can become excessively large in magnitude and possibly damage the object and arms structure, if ignored in resolving the torque redundancy in (10). As illustrated in the simulation experiments, the minimization of constraint force presented here directly minimizes the squeeze force, with no influence on the motion-inducing part.

### C. Practical Consideration

There might be situations in which the dynamics properties of the object to be manipulated are unknown, e.g., in search and rescue scenarios. In this section, we discuss how the developed method can be adapted to such situations by applying time-delayed estimation technique [17]. We assume no information about the object is given, unless its undeformability, and the grasp points position, which can indeed be calculated from the arms forward kinematics due to the rigid grasping assumption. Moreover, for easy presentation we develop the estimations for the case of minimizing costs in the control command, i.e., with $\tau_0 = 0$.

Recalling the proposed constrained representation (8) and (6), one can observe that only $\hat{M}$ and $\hat{h}$ include object dynamics terms that can affect the derivations. Note that $J_{\mathrm{g}}$ will not be affected, because

$$G_{\mathrm{oa}}G_{\mathrm{ob}}^{-1} = \begin{bmatrix} I & p_{o/a}\times \\ 0 & I \end{bmatrix}\begin{bmatrix} I & -p_{o/b}\times \\ 0 & I \end{bmatrix} = \begin{bmatrix} I & (p_{o/a}\times) - (p_{o/b}\times) \\ 0 & I \end{bmatrix},$$

is independent of the object's CoM position. We shall now rewrite $\hat{M}$ and $\hat{h}$ as

$$\hat{M} = M + J_{\mathrm{b}}^T \mathcal{M}_1 J_{\mathrm{b}},$$
$$\hat{h} = h + J_{\mathrm{b}}^T \mathcal{M}_2,$$

with

$$\mathcal{M}_1 = G_{\mathrm{ob}}^{-\mathrm{T}} M_{\mathrm{o}} G_{\mathrm{ob}}^{-1},$$
$$\mathcal{M}_2 = G_{\mathrm{ob}}^{-\mathrm{T}} \left( h_{\mathrm{o}} + M_{\mathrm{o}} G_{\mathrm{ob}}^{-1} \left( \dot{J}_{\mathrm{b}} - \dot{G}_{\mathrm{ob}} G_{\mathrm{ob}}^{-1} J_{\mathrm{b}} \right) \dot{q} \right),$$

being the affected terms by the object dynamics. Subsequently, the inverse dynamics equation (10) can be rewritten as

$$\tau(W, \tau_0) = \left(PS^{\mathrm{T}}\right)^{\#} P\big( \left(M + J_{\mathrm{b}}^T \bar{\mathcal{M}}_1 J_{\mathrm{b}}\right) \ddot{q}_{\mathrm{des}} + h + J_{\mathrm{b}}^T \mathcal{M}_2 + J_{\mathrm{b}}^T \left(\mathcal{M}_1 - \bar{\mathcal{M}}_1\right) J_{\mathrm{b}} \ddot{q}_{\mathrm{des}} \big), \tag{17}$$

in which $\bar{\mathcal{M}}_1$ is a rough estimation of $\mathcal{M}_1$. To calculate it, we specify $\bar{M}_{\mathrm{o}}$ with some rough estimation of the object inertial parameters in the main diagonal and zero elsewhere, and estimate $\bar{J}_{\mathrm{ob}}$ by assuming an approximate position for the object's CoM.

Now let $\mathcal{H}$ includes all the terms containing unknown dynamic parameters:

$$\mathcal{H} = \left(PS^{\mathrm{T}}\right)^{\#} P \left( J_{\mathrm{b}}^T \mathcal{M}_2 + J_{\mathrm{b}}^T \left(\mathcal{M}_1 - \bar{\mathcal{M}}_1\right) J_{\mathrm{b}} \ddot{q}_{\mathrm{des}} \right). \tag{18}$$

We estimate $\mathcal{H}$ with its known value from the previous time step, that is, time-delayed estimation [17], [18] given as

$$\mathcal{H}_{(t)} \approx \mathcal{H}_{(t-L)} \approx \{\tau - \left(PS^{\mathrm{T}}\right)^{\#} P \left( \left(M + J_{\mathrm{b}}^T \bar{\mathcal{M}}_1 J_{\mathrm{b}}\right) \ddot{q} + h \right)\}_{(t-L)}. \tag{19}$$

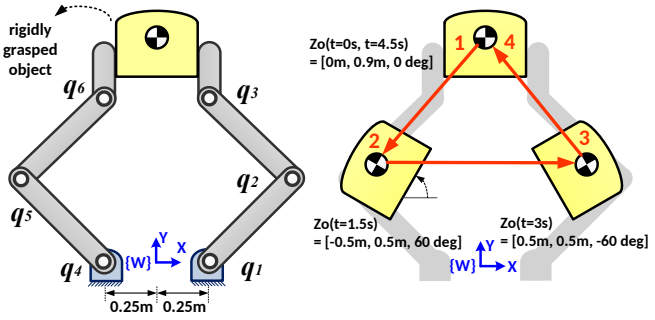


Fig. 2. Planar bimanual object manipulation system, and the reference task properties.

When the time step $L$ is sufficiently small (e.g., $L = 5\,\mathrm{ms}$ used in this paper), this enables the object model-free computation of the control command as

$$\tau(W, \tau_0) \approx \left(PS^{\mathrm{T}}\right)^{\#} P \left( \left(M + J_{\mathrm{b}}^T \bar{\mathcal{M}}_1 J_{\mathrm{b}}\right) \ddot{q}_{\mathrm{des}} + h \right) + \mathcal{H}_{(t-L)}. \tag{20}$$

Having determined $\tau$, one can solve (14) for the constraint force $\lambda$. The effectiveness of this inverse dynamics control with time-delayed estimation, i.e., an object model-free control, is demonstrated via simulation experiments in the following section.

## IV. Simulation Experiments

In this section, we implement the developed inverse dynamics control in simulation on a planar bimanual object manipulation model composed of two identical 3-link manipulators (see Fig. 2). Actuation is assumed possible for all joints, hence, $S = I_6$. Both full model-based and object model-free methods are explored, and the performance when different quadratic costs are minimized is illustrated. Two cases are considered:

- **case 1**: the minimization of the quadratic cost $\frac{1}{2}\tau^{\mathrm{T}} W_\tau \tau$, with $W = I_6$ (see Section III-B.1);
- **case 2**: the minimization of the quadratic cost $\frac{1}{2}\lambda^{\mathrm{T}} W_\lambda \lambda$, with $W_\lambda = I_6$ (see Section III-B.2).

The object mass and moment of inertia are chosen as $m_{\mathrm{o}} = 2\,\mathrm{kg}$ and $I_{zzo} = 0.0142\,\mathrm{kg.m}^2$. For the similar arms we set $m_1 = m_2 = 1.5\,\mathrm{kg}$, $m_3 = 1\,\mathrm{kg}$, $l_1 = l_2 = 0.4\,\mathrm{m}$, and $l_3 = 0.15\,\mathrm{m}$. Each link's CoM position is in the mid-length of the link, and the moment of inertias are calculated assuming cubic link geometry with the surface area of $w \times w$ with $w = 0.1\,\mathrm{m}$. The arms start from reset with the joint positions of $q_0 = \begin{bmatrix} \frac{\pi}{3} & \frac{\pi}{3} & -\frac{\pi}{3} & \frac{2\pi}{3} & -\frac{\pi}{3} & \frac{\pi}{3} \end{bmatrix}^{\mathrm{T}}$, and the corresponding object position is $z_{o,0} = \begin{bmatrix} x & y & \theta \end{bmatrix}^{\mathrm{T}} = \begin{bmatrix} 0 & 0.9 & 0 \end{bmatrix}^{\mathrm{T}}$.

The task is to control the object to follow a path forming a triangle with the desired object states at its corners as illustrated in Fig. 2. To do so, piecewise fifth order polynomials are used to express the reference position trajectories, $z_{\mathrm{o,des}}(t)$, in task space. At each time step, the following relation is then used to obtain the constraint consistent joint

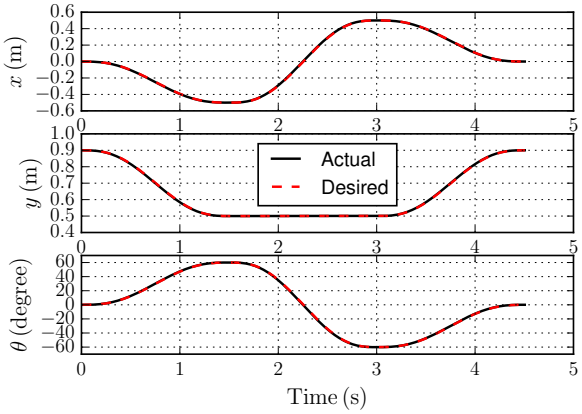


Fig. 3. Position tracking of the object's CoM.

accelerations:

$$\ddot{q}_{\mathrm{des}} = \begin{bmatrix} J_{\mathrm{g}} \\ G_{\mathrm{ob}}^{-1} J_{\mathrm{b}} \end{bmatrix}^{+} \left( \begin{bmatrix} 0 \\ a \end{bmatrix} - \begin{bmatrix} \dot{J}_{\mathrm{g}} \\ G_{\mathrm{ob}}^{-1} \left( \dot{J}_{\mathrm{b}} - \dot{G}_{\mathrm{ob}} G_{\mathrm{ob}}^{-1} J_{\mathrm{b}} \right) \end{bmatrix} \dot{q} \right), \tag{21}$$

in which

$$a = \dot{v}_{\mathrm{o,des}} + k_{\mathrm{d}} \left( v_{\mathrm{o,des}} - v_{\mathrm{o}} \right) + k_{\mathrm{p}} \left( z_{\mathrm{o,des}} - z_{\mathrm{o}} \right),$$

with $k_{\mathrm{p}}$ and $k_{\mathrm{d}}$ being some positive definite matrices. The total simulation time of $4.5\,\mathrm{s}$ is equally distributed for the three sides of the triangle, and the control loop runs at a $200\,\mathrm{Hz}$ rate. The simulations were carried out in Python 2.7, where standard routines of Scipy were used for the computation of control policies as well as the forward dynamics.

### A. Simulation results

Fig. 3 shows the object position variables together with the corresponding desired values. Note that the results are the same for both case 1 and case 2. The inverse dynamics torques of the right arm for case 1 and case 2 are depicted in Figs. 4 and 5, respectively. The corresponding RMS values of the motion-inducing and squeeze force are shown in Figs. 6 and 7, respectively. Note that the instantaneous value of squeeze forces for the two arms would clearly be the same but with different signs.

In order to evaluate the object model-free controller proposed in Section III-C, we repeat the simulation in case 1 with the control policy (20). In doing so we approximate the object inertia matrix as $\bar{M}_{\mathrm{o}} = \mathrm{diag}(1\,\mathrm{kg}, 1\,\mathrm{kg}, 0.1\,\mathrm{kg.m}^2)$, and its position to be equally distanced from the known grasp points. Fig 8 and 9 depict the object position tracking and constraint force prediction errors, respectively. In the latter figure, only the results of the right arm are shown for clarity.

### B. Discussions

The manipulation of an undeformable object with proper control over joint torques and/or constraint forces has been realized in a computationally efficient framework that does not need constraint force measurement. Fig. 3 presents that

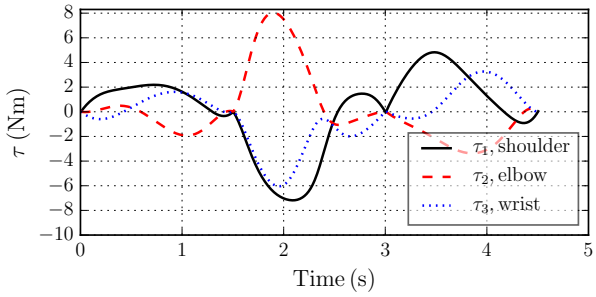


Fig. 4. The right arm torque profiles for case 1.

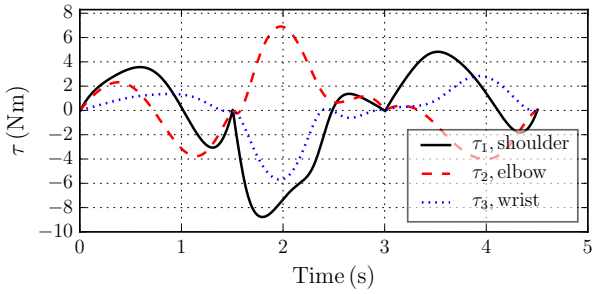


Fig. 5. The right arm torque profiles for case 2.

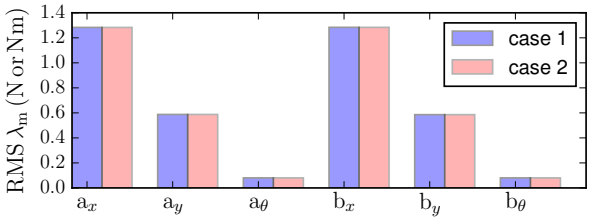


Fig. 6. RMS values of the motion-inducing constraint force when minimizing a quadratic cost in control command (case 1) and constraint force (case 2).

the desired position is precisely tracked, and the required control commands shown in Figs. 4 and 5 are fairly smooth and practically feasible. One can see that required torques in case 1 are slightly smaller than case 2 (more precisely, the magnitude of $\tau^{\mathrm{T}}\tau$ at each time step is smaller). Nevertheless, the main difference can particularly be seen in Fig. 7, where the squeeze forces are dramatically influenced after minimizing the cost in $\lambda$ (case 2). As outlined earlier, the motion-inducing forces remain the same for the two cases shown in Fig. 6, and the minimization only affects the squeeze forces.

Note that this is just an example test. Depending on the particular setup and the task at hand, one may not want to minimize the whole squeeze force, but only the tangential components to avoid slippage. This can be realized by defining a proper weighting matrix $W_{\lambda}$. Moreover, if having box constraints on the value of control command and/or constraint force is critically important for a particular application, one can reformulate the control calculation to a quadratic programming with respective inequality con-

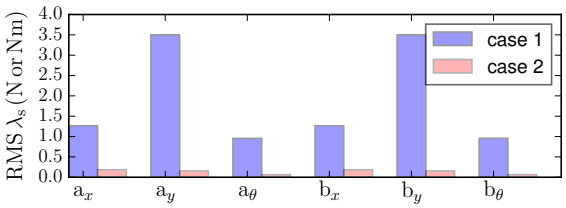


Fig. 7. RMS values of the internal (squeeze) constraint force when minimizing a quadratic cost in control command (case 1) and constraint force (case 2).

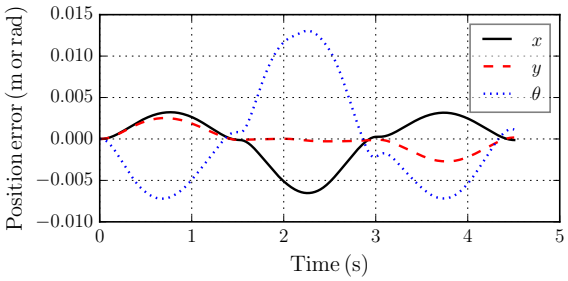


Fig. 8. Position tracking errors when time-delayed estimation is used for the dynamics parameters of the object.

straints [15].

As for the object model-free simulations, observe that the position tracking error, depicted in Fig. 8, remains remarkably small, albeit no knowledge of the object dynamics properties is assumed and no force measurement of any kind is used. We have successfully implemented this sort of time-delayed estimations on real platforms in other robotic applications already [18]. One final comment on the constraint force prediction (Fig. 9) is that the least accuracy, presented in the $y$ component, corresponds to a $24.6\%$ error. We note that by increasing the loop frequency, this could significantly decrease. For example, increasing the loop rate to $1\,\mathrm{kHz}$, which is manageable by state-of-the-art robotic hardware setups, would decrease the intended error to $7.1\%$.

## V. Conclusion

A force sensor-less and computationally efficient inverse dynamics control for the bimanual manipulation of undeformable objects has been addressed in this paper. To the best of authors' knowledge, the presented method provides the first analytically correct solution to the inverse dynamics of such systems. We presented a compact formulation for the bimanual manipulation dynamics that admits available decomposition techniques. This work has been developed towards introducing a unified framework for the whole body control of the under development robot CENTAURO, which is intended to perform bimanual manipulation with an anthropomorphic upper-body mounted on a quadrupedal lower-body.

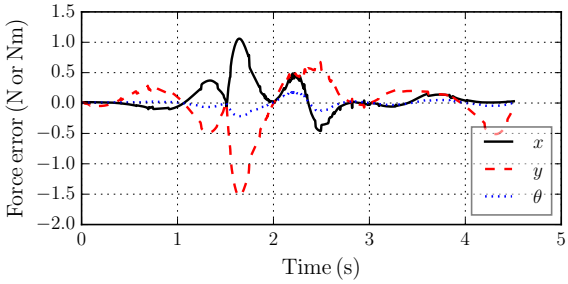


Fig. 9. Constraint force prediction errors when time-delayed estimation is used for the dynamics parameters of the object.

## References


[1] M. Uchiyama and P. Dauchez, "A symmetric hybrid position/force control scheme for the coordination of two robots," in *Robotics and Automation, 1988. Proceedings., 1988 IEEE International Conference on*. IEEE, 1988, pp. 350–356.

[2] W.-H. Zhu and J. De Schutter, "Control of two industrial manipulators rigidly holding an egg," *IEEE control systems*, vol. 19, no. 2, pp. 24–30, 1999.

[3] F. Caccavale, P. Chiacchio, A. Marino, and L. Villani, "Six-dof impedance control of dual-arm cooperative manipulators," *IEEE/ASME Transactions On Mechatronics*, vol. 13, no. 5, pp. 576–586, 2008.

[4] C. Smith, Y. Karayiannidis, L. Nalpantidis, X. Gratal, P. Qi, D. V. Dimarogonas, and D. Kragic, "Dual arm manipulationa survey," *Robotics and Autonomous systems*, vol. 60, no. 10, pp. 1340–1353, 2012.

[5] A. M. Okamura, N. Smaby, and M. R. Cutkosky, "An overview of dexterous manipulation," in *Robotics and Automation, 2000. Proceedings. ICRA'00. IEEE Int. Conf. on*, vol. 1. IEEE, 2000, pp. 255–262.

[6] V. Kumar and J. F. Gardner, "Kinematics of redundantly actuated closed chains," *IEEE Transactions on Robotics and automation*, vol. 6, no. 2, pp. 269–274, 1990.

[7] A. Bicchi, "Hands for dexterous manipulation and robust grasping: A difficult road toward simplicity," *IEEE Transactions on robotics and automation*, vol. 16, no. 6, pp. 652–662, 2000.

[8] M. A. Unseren, "A review of a method for dynamic load distribution, dynamical modeling, and explicit internal force control when two manipulators mutually lift and transport a rigid body object," Oak Ridge National Lab., TN (United States), Tech. Rep., 1997.

[9] T. Yoshikawa and X.-Z. Zheng, "Coordinated dynamic hybrid position/force control for multiple robot manipulators handling one constrained object," *The International Journal of Robotics Research*, vol. 12, no. 3, pp. 219–230, 1993.

[10] R. Bonitz and T. C. Hsia, "Internal force-based impedance control for cooperating manipulators," *IEEE Transactions on Robotics and Automation*, vol. 12, no. 1, pp. 78–89, 1996.

[11] F. Aghili, "A unified approach for inverse and direct dynamics of constrained multibody systems based on linear projection operator: applications to control and simulation," *IEEE Transactions on Robotics*, vol. 21, no. 5, pp. 834–849, 2005.

[12] M. Mistry, J. Buchli, and S. Schaal, "Inverse dynamics control of floating base systems using orthogonal decomposition," in *Robotics and Automation (ICRA), 2010 IEEE International Conference on*. IEEE, 2010, pp. 3406–3412.

[13] L. Sciavicco and B. Siciliano, *Modeling and control of robot manipulators*. McGraw-Hill New York, 1996, vol. 8, no. 0.

[14] L. Sentis and O. Khatib, "Synthesis of whole-body behaviors through hierarchical control of behavioral primitives," *International Journal of Humanoid Robotics*, vol. 2, no. 04, pp. 505–518, 2005.

[15] L. Righetti, J. Buchli, M. Mistry, M. Kalakrishnan, and S. Schaal, "Optimal distribution of contact forces with inverse-dynamics control," *The Int. J. of Robotics Research*, vol. 32, no. 3, pp. 280–298, 2013.

[16] H. Flashner, "An orthogonal decomposition approach to modal synthesis," *International journal for numerical methods in engineering*, vol. 23, no. 3, pp. 471–493, 1986.

[17] K. Youcef-Toumi and O. Ito, "A time delay controller for systems with unknown dynamics," *Journal of dynamic systems, measurement, and control*, vol. 112, no. 1, pp. 133–142, 1990.

[18] J. Lee, H. Dallali, N. Tsagarakis, and D. Caldwell, "Robust and model-free link position tracking control for humanoid coman with multiple compliant joints," in *Humanoid Robots (Humanoids), 2013 13th IEEE-RAS International Conference on*. IEEE, 2013, pp. 1–7.